High-pressure and magneto-optical studies of Cr-related defects in the lithium-rich $LiNbO_3$:Cr,Mg crystal

A. Kamińska, A. Suchocki, and S. Kobyakov
Institute of Physics, Polish Academy of Sciences, Aleja Lotników 32/46, 02-668 Warsaw, Poland

L. Arizmendi
Departamento de Fisica de Materiales, Universidad Autonoma de Madrid, Cantoblanco, 28049 Madrid, Spain

M. Potemski and F. J. Teran*
Grenoble High Magnetic Field Laboratory, CNRS, 25 Avenue des Martyrs, Boîte Postale 166, 38042 Grenoble, France
(Received 11 May 2007; published 30 October 2007)

In this paper we present spectroscopic data clarifying the nature of the Cr^{3+} centers and Cr^{3+}-related defect in the $LiNbO_3$:Cr,Mg crystal containing an excess of Li^+ ions. Apart from quite well known lines associated with the $^4T_2 \rightarrow {}^4A_2$ and $^2E \rightarrow {}^4A_2$ transitions of the Cr^{3+} ions, the luminescence spectrum of this crystal reveals some additional relatively narrow lines in the range of 750–860 nm. We carried out high-pressure and magneto-optical measurements of the crystallographically oriented samples of this crystal at temperature of 10 K. The measured spectra, decay times, pressure coefficients, and the dependence of the luminescence on high magnetic field show that the luminescence lines observed in lithium-rich $LiNbO_3$:Cr,Mg originate from both Cr^{3+} ions and strongly antiferromagnetically coupled Cr^{3+}-Cr^{3+} first nearest-neighbor pairs. The ground-state levels of the pairs can be described by the isotropic exchange interaction $\mathcal{H}=J\boldsymbol{S}_1\cdot\boldsymbol{S}_2+j(\boldsymbol{S}_1\cdot\boldsymbol{S}_2)^2$, where $\boldsymbol{S}_1$ and $\boldsymbol{S}_2$ are the total spins of each of the two chromium ions. The obtained results enabled us to determine the ground-state spin-spin exchange constants J and j as well as the excited-state zero field splitting constant D.

DOI: 10.1103/PhysRevB.76.144117 PACS number(s): 78.20.−e, 77.84.−s, 71.70.Ej, 07.35.+k

I. INTRODUCTION

Lithium niobate (LN) crystals remain of great interest for applications as well as for fundamental studies. This material is one of the most important for application in nonlinear optics.[1] The significant advantage of this material is that it can be relatively easy doped with various transition metal and rare earth ions and that its physical properties are strongly sensitive to the crystal composition and defect structure. $LiNbO_3$ doped with $Fe^{2+/3+}$, $Mn^{2+/3+}$, or $Cu^{1+/2+}$ is a very good crystal for holographic recording and then the potential material for high-capacity optical memory. This compound with various dopants exhibits also very interesting piezoelectric, electroacoustic, and electro-optic features which allow using it for waveguides (for instance, with the Ti^{3+} dopant), electro-optical devices, integrated optics, and ultrasonic technics. $LiNbO_3$ doped with neodymium is an efficient lasing medium which can be used for self-frequency doubling lasers.

The defect structure of this crystal is still one of the main subjects of research. The Cr^{3+} ions turned out to be a very good probe of that structure since they substitute for both Li and Nb ions in the LN host. Additionally their physical properties are strongly sensitive to crystal composition and defect structure. In the past the Cr^{3+} centers in $LiNbO_3$ have been a subject of intense debate, which was partly caused by the intrinsic Li^+ deficit which affects the Cr ions and intrinsic defects distribution. Various optical studies as well as those with the use of electron paramagnetic resonance (EPR) and electron-nuclear double resonance techniques have been performed, which helped us to identify several Cr^{3+} centers both in Li (Cr_{Li}) and Nb (Cr_{Nb}) sites and to determine conditions which influence the distribution of Cr^{3+} ions between these sites.[2–4] Also high-pressure low-temperature optical spectroscopy was very successful in identification of optically active Cr^{3+} centers.[5–7] Application of high hydrostatic pressure reduces the distances between the ion and the ligands. Thus it increases the strength of the crystal field experienced by the Cr^{3+} ions and as a result—the energy of the $^4T_2$ state, which in the case of low-strength crystal field is the first excited state of this ion. When the ion environment is transformed into the high-strength crystal field—the ^2E level becomes the first excited state, which luminescence lines associated with the $^2E \rightarrow {}^4A_2$ transitions have the width 10–100 times smaller than the broadband luminescence associated with the $^4T_2 \rightarrow {}^4A_2$ transitions. This reduces difficulties in the interpretation of the overlapping spectra emitted by different centers. In this way chromium centers in congruent and near-stoichiometric crystals of $LiNbO_3$:Cr and $LiNbO_3$:Cr,MgO crystals have been spectrally resolved.[5–7]

The main purpose of this work is the investigation of intrinsic defects and dopant center structure in the $LiNbO_3$:Cr,MgO crystal containing an excess of Li^+ ions. Apart from quite well known lines associated with the $^4T_2 \rightarrow {}^4A_2$ and $^2E \rightarrow {}^4A_2$ transitions of the Cr^{3+} ions, the luminescence spectrum of this crystal reveals some additional relatively narrow lines in the range of 750–790 nm and a group of broader lines in the range of 790–860 nm. Some of these lines were observed also by other authors (Basun *et al.*,[8] Salley *et al.*,[9] and Trepakov *et al.*[10]) and were attributed to an exchange-coupled pair involving at least one Cr^{3+} ion (most probably Cr^{3+}-Cr^{3+} or Cr^{3+}-Nb^{4+} pair).

We report the results of pressure dependence and magneto-optical measurements of Cr^{3+} luminescence of Li-

excess $LiNbO_3$ crystal doped with chromium and codoped with MgO. It will be shown that all these additional lines are related to the center formed by the Cr^{3+}-Cr^{3+} pairs.

II. EXPERIMENT

As it was mentioned yet, formerly growing and intensively investigated $LiNbO_3$ crystals were the congruent ones, in which the ratio [Li]/[Nb]=48.6/51.4. In the late 1980s near-stoichiometric crystals, in which [Li]/[Nb]≈1/1, were obtained by several methods.[11] Lately, the crystals with lithium ion excess have been obtained in the Crystal Growth Laboratory of the Department of Physics of Materials of Universidad Autonoma de Madrid. The samples used in these studies have been grown by high-temperature top seeded solution growth method at this university from a melt to which about 4% of K_2O has been added. Lithium in a concentration of 58 mol %, chromium in a concentration of 0.4 mol %, and magnesium in a concentration of 1 mol % have been also added to the melt. The Li/Nb ratio in the melt was about 1.4. The obtained sample was violet brown; unlikely both $LiNbO_3$ crystals with characteristic green color contained chromium ions in the Li sites and those pink in color, where the Cr^{3+} ions are located, mainly in the Nb sites.[7]

The absorption spectra have been measured on a Hitachi U3501 spectrophotometer. The sample was placed into the closed-cycle cryostat for low-temperature measurements.

Continuous wave emission spectra were obtained using a 514.5 nm line of an argon-ion laser as the excitation source. Details of the high-pressure diamond-anvil cell (DAC) experimental setup can be found elsewhere.[7]

All the magneto-optical measurements were performed in Grenoble High Magnetic Field Laboratory. Substantial size of resistive magnet providing high magnetic fields imposed the use of fiber optics in such experiments. The laser excitation (Ar^+ laser working in the multiline mode) was led to the sample via the first fiber and focused by a combination of two microlenses. The emission signal was collected by the second fiber, analyzed by a 1 m double grating monochromator, and detected by a liquid nitrogen cooled charge-coupled device camera. The setup was placed in the liquid helium insert of a cryostat at $T \approx 5$ K and the cryostat located in a resistive magnet supplying magnetic field up to 23 T. There were measured the polarization resolved photoluminescence spectra of two differently oriented samples (one z cut and the other x cut) of the crystal in both Faraday and Voigt configurations.

III. RESULTS AND DISCUSSION

A. Absorption and luminescence spectra of bulk Li-rich $LiNbO_3$:Cr,MgO crystal at ambient pressure

The low-temperature absorption spectrum of the $LiNbO_3$:Cr^{3+},MgO crystal with excess of Li^+ ions is presented in Fig. 1. For comparison the figure includes also the low-temperature absorption spectrum of the stoichiometric $LiNbO_3$:Cr^{3+} (dashed lines) and $LiNbO_3$:Cr^{3+},MgO (dotted lines) crystals.[7] The spectra of the Li-rich and stoichiometric

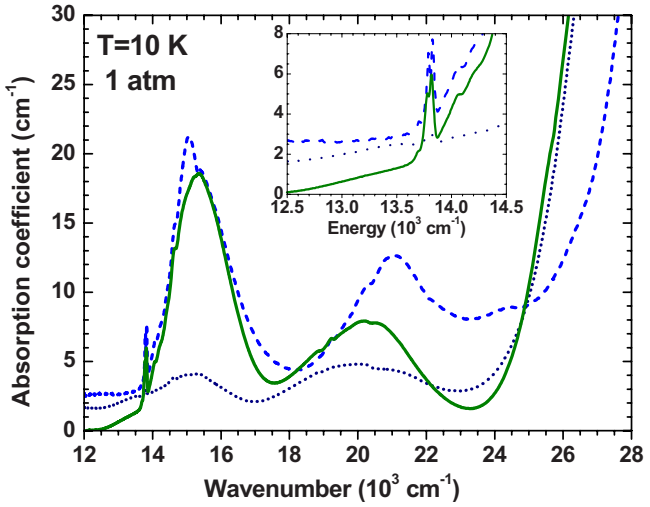

FIG. 1. (Color online) Absorption spectra of $LiNbO_3$:Cr^{3+},MgO crystal containing excess of Li^+ ions (solid lines), stoichiometric $LiNbO_3$:Cr^{3+} (dashed lines), and stoichiometric $LiNbO_3$:Cr^{3+},MgO (dotted lines) measured at temperature $T=10$ K at ambient pressure. Inset: expanded spectra in the region of the R lines.

$LiNbO_3$:Cr^{3+} crystals exhibit strong and sharp R lines associated with the γ and β Cr^{3+} centers (according to the notation introduced in Ref. 2) which correspond to nonequivalent Cr^{3+} ions in Li^+ sites. On the other side, the broadband structures as well as the absorption edge of the Li-rich crystal are observed at similar energy values like in the $LiNbO_3$:Cr^{3+},MgO crystal in which the center δ corresponding to Cr^{3+} ions in Nb^{5+} sites dominates. Therefore we conclude that in the $LiNbO_3$:Cr^{3+},MgO crystal containing the excess of Li^+ ions the distribution of the chromium ions between Li^+ sites and Nb^{5+} sites is more balanced than in previously studied near-stoichiometric crystals and could allow us to observe Cr^{3+}-Cr^{3+} chromium pairs in lithium niobate.

Low-temperature luminescence spectrum of the $LiNbO_3$:Cr^{3+},MgO crystal containing an excess of Li^+ ions is presented in Fig. 2. Like in the case of absorption, the figure includes for comparison the low-temperature luminescence spectra of the stoichiometric $LiNbO_3$:Cr^{3+} (dashed lines) and $LiNbO_3$:Cr^{3+},MgO (dotted lines) crystals.[7] In addition to the well known features of the $LiNbO_3$:Cr^{3+} and $LiNbO_3$:Cr^{3+},MgO spectra,[2,7] the spectrum of Li-rich $LiNbO_3$:Cr^{3+},MgO crystal shows a set of lines in the wavelength region from 758 to 855 nm (the wave number region from 11 700 to 13 190 cm^{-1}; 8065 cm^{-1}=1 eV). These lines exhibit a dependence of intensity on the sample orientation and a strong π polarization, which is presented in Figs. 3(a) and 3(b).

Lines 1–3 from Fig. 3(b) were observed and described earlier in many $LiNbO_3$ crystals containing chromium dopant. They are associated with the $^4T_2 \rightarrow {}^2E$ transitions of the Cr^{3+} centers visible at ambient pressure as follows.[2,7,12]

(1) The line at 13 683 cm^{-1} (730.8 nm) is related to the so called β center created by the Cr^{3+} ions in the lithium crystal site (distorted octahedral site).

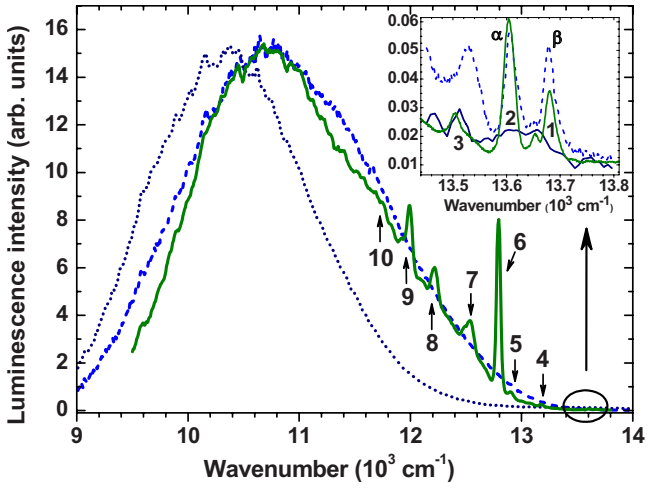

FIG. 2. (Color online) Luminescence spectra of $LiNbO_3:Cr^{3+},MgO$ crystal containing excess of Li^+ ions (solid lines), stoichiometric $LiNbO_3:Cr^{3+}$ (dashed lines), and stoichiometric $LiNbO_3:Cr^{3+},MgO$ (dotted lines) measured at temperature $T=10$ K at ambient pressure, excited by the 514.5 nm argon-ion laser line. Inset: expanded spectra in the region of the R lines. Lines 1–10 are described in the text.

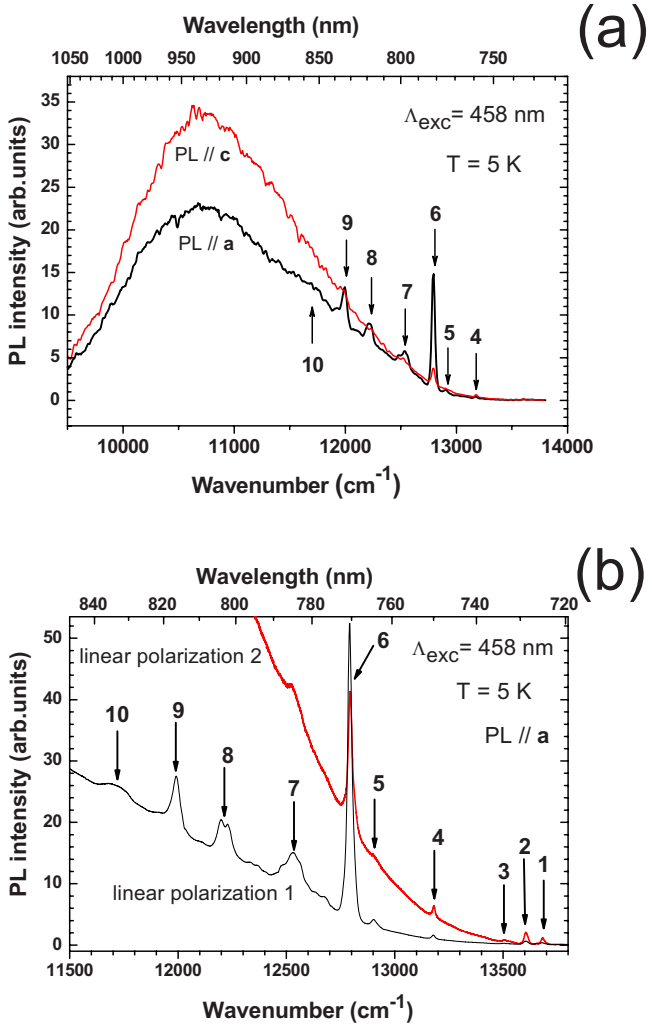

FIG. 3. (Color online) The dependence of luminescence of $LiNbO_3:Cr^{3+},MgO$ crystal containing excess of Li^+ ions on (a) the orientation of the sample: PL$\|a$ and PL$\|c$ means photoluminescence collected along the c and a axes of the crystal, respectively, and (b) the excitation polarization: linear polarization 1 means the polarization of the excited light, at which lines 5–10 were the most intensive and linear polarization 2 means the polarization of the excited light perpendicular to the polarization 1. All the spectra were measured at 5 K under excitation at 458 nm. Lines 1–10 are described in the text.

(2) The line at 13 605 cm^{-1} (735 nm) is related to the so called α center created by the Cr^{3+} ions in the lithium crystal site (the second type of distorted octahedral site).

(3) The line at 13 507 cm^{-1} (740.4 nm) is related to the so called ε center created by the Cr^{3+} ions in the niobium crystal site (almost undistorted octahedral site).

Lines or groups of lines 6–10 from Fig. 3(b) were also observed by Basun *et al.*,[8] Salley *et al.*,[9] and Trepakov *et al.*,[10] and were attributed by the authors to an exchange-coupled pair involving at least one Cr^{3+} ion (most probably Cr^{3+}-Cr^{3+} or Cr^{3+}-Nb^{4+} pair). These lines peak at the following wave numbers: line 6—12 795 cm^{-1} (781.6 nm), line 7—about 12 530 cm^{-1} (798.1 nm)—actually the overlapped group of 3 or even more lines, line 8—12 232 and 12 198 cm^{-1} (817.5 and 819.8 nm)—actually the pair of lines, line 9—11 993 cm^{-1} (833.8 nm), and line 10—11 726 cm^{-1} (852.8 nm).

We also observed in the spectra two weak lines marked in Fig. 3 as 4 (13 181 cm^{-1} or 758.7 nm) and 5 (12 904 cm^{-1} or 775.0 nm).

We have measured the decay kinetics of lines 6–9 at the temperature $T=10$ K (see Fig. 4). They all are single exponential. Lines 6–8 exhibit the same decay time equal to 39 μs (±2 μs in the case of line 6 and ±4 μs in the case of lines 7 and 8), which suggests the same origin of these lines. The decay time of line 9 is equal to 31±2 μs. These values are different from both the decay times of the narrow R lines associated with the single Cr^{3+} ions, which are in the range exceeding 200 μs and the decay time of the broadband background equal to 9±1 μs.[7] The value of the decay time of lines 6–8 is similar to the value of 43 μs reported by Basun *et al.*[8] who have studied the 770–850 nm (11 800–13 000 cm^{-1}) lines. Such results are consistent with respective values of decay times measured for chromium pairs in ruby[13–15] and lanthanum aluminate,[16] which are also several times smaller than the decay times of respective R lines.

The temperature dependencies of the spectra in the region 11 800–13 100 cm^{-1} are presented in Fig. 5 and the relative luminescence intensities of lines 9 and 6 versus inverse temperature in Fig. 6. At elevated temperature the proportion of the luminescence intensity of line 9 to the luminescence intensity of the strongest line 6 decreases up to about 80 K and then it increases. This fact indicates that the thermal equilibrium of the populations of the excited levels occurs over 80 K only. Similar behavior was observed by Powell and DiBartolo who studied chromium pairs in ruby.[14]

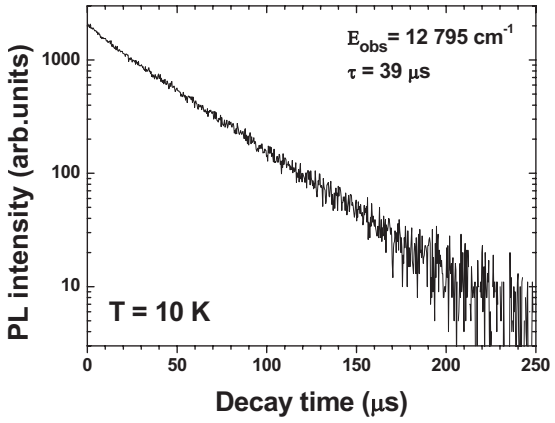

FIG. 4. Luminescence decay kinetics of $LiNbO_3:Cr^{3+},MgO$ crystal containing excess of Li^+ ions measured at the energy 12 795 cm^{-1} and $T=10$ K.

The measured decay times as well as temperature behavior of the spectrum allow us to suppose that the set of lines 4–10 can be related with the chromium pairs present in the lithium niobate crystal lattice. The capability of creating self-compensated pairs of chromium ions occupying neighboring lithium and niobium positions which likewise have trigonal point group symmetry C_3 was studied theoretically by Yeom *et al.*[17] and experimentally (on the crystal doped with 0.8 wt % chromium) by Siu *et al.*[18] The ground state of such pair $({}^4A_2+{}^4A_2)$ consists of four levels with total spins $S=0,1,2,3$ and the first excited state $({}^4A_2+{}^2E)$ consists of two levels with total spins $S'=1,2$.

At temperatures higher than 80 K the experimental data can be fitted to Boltzmann exponential $e^{-\Delta E/kT}$, where ΔE is the energy difference between the excited states, from which the transitions occur. In the case of chromium pair this is the difference between the levels with $S'=2$ and $S'=1$. From the fit to the experimental data we obtained ΔE equal to 58 ± 8 cm^{-1}.

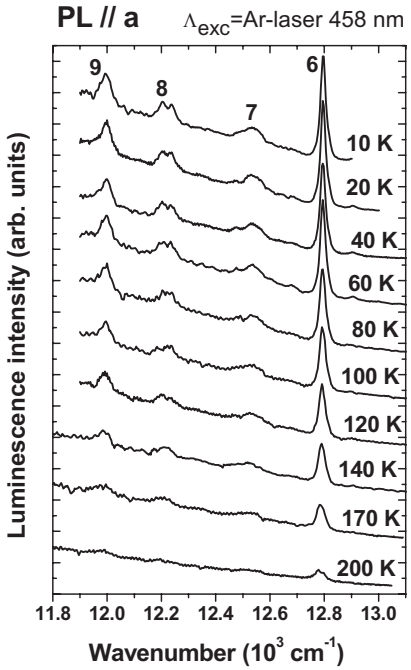

FIG. 5. The temperature dependence of lines 6–9 in the $LiNbO_3:Cr^{3+},MgO$ crystal containing excess of Li^+ ions measured at ambient pressure. PL$\|a$ means the same as in Fig. 3.

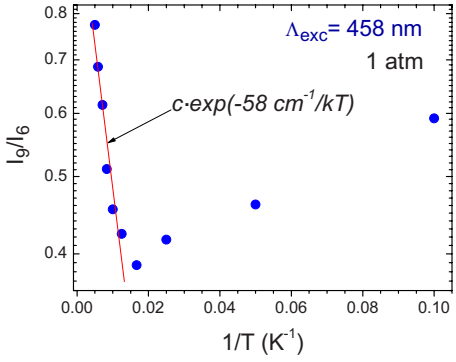

FIG. 6. (Color online) The temperature dependence of the relative luminescence intensities of lines 9 (11 993 cm^{-1}) and 6 (12 795 cm^{-1}). ΔE in the exponential is given in cm^{-1}.

B. Pressure dependence of luminescence spectra at low temperature

Apart from the most intensive line 6 (12 795 cm^{-1}) no other sharp lines are observed in the spectrum of the sample measured in the DAC at low pressure. This is due to low luminescence intensity of the lines observed using much larger samples than is possible to load into DAC. However, application of pressure changes considerably the luminescence spectrum of the crystal. Examples of the spectra of the examined crystal at a temperature of 10 K are presented in Fig. 7. At a pressure of about 12 kbar the R_1 lines of the well known β and γ centers (both created by the Cr^{3+} ions in the

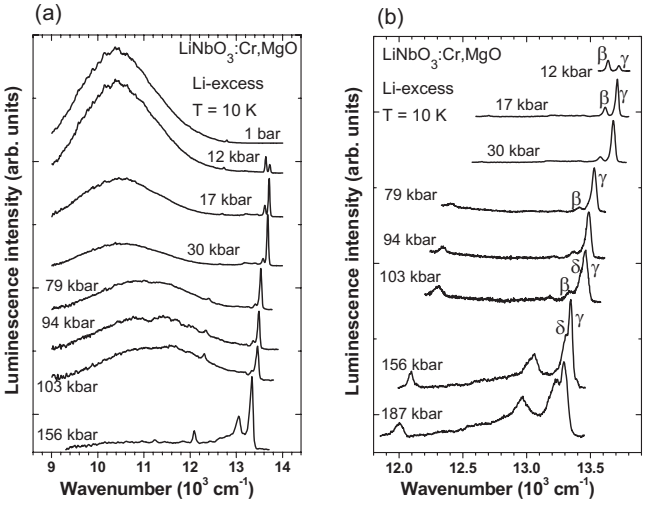

FIG. 7. The pressure dependence of the Cr^{3+} luminescence in Li-rich $LiNbO_3:Cr,MgO$ crystal at temperature $T=10$ K: (a) the whole spectrum, and (b) the spectrum in the region of the R lines and the $1'\rightarrow1$ transition of the Cr^{3+}-Cr^{3+} pairs.

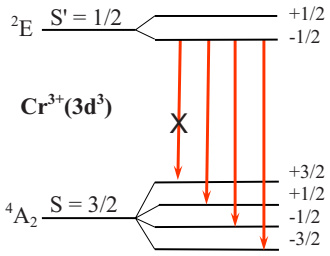

FIG. 8. (Color online) Zeeman splitting of the R_1 line of single Cr^{3+} ion in the external magnetic field. At low temperature all the excited electrons thermalize at the same spin polarization. The spin forbidden transition is marked by the crossed arrow.

lithium crystal site)[1,6] became clearly visible since the increase of pressure increases the energy of the $^4T_2$ level and the ^2E level became the first excited state of Cr^{3+} ions occupying these two centers. At higher pressures, beginning from 90 kbar, an additional sharp line becomes discernible in the spectra in between the β and γ centers. This is R_1 line associated with the δ center created by the Cr^{3+} ions in the niobium crystal site.[2,7] The increase of the intensity of the $R_1(\gamma)$ and $R_1(\delta)$ lines proceeds at the expense of the broadband luminescence, associated with the $^4T_2 \rightarrow {}^4A_2$ transitions of the Cr^{3+} ions in the γ and δ centers. The pressure behavior of the luminescence lines associated with these centers has been described in detail in Ref. 7. The pressure coefficients of the position of the R_1 lines of γ and δ centers are equal to −2.9 and −1.8 cm^{-1}/kbar, respectively. The interception points with the energy axis at ambient pressure are equal to 13 770±2 and 13 628±6 cm^{-1}, respectively.

Other lower energy and smaller intensity lines, visible at higher pressures, are the phonon replicas of the R_1 lines of the main γ and δ centers.

The peak position of the broadband luminescence also depends on pressure and its pressure coefficient is equal to +11 cm^{-1}/kbar, similarly to the pressure coefficient measured in the near-stoichiometric $LiNbO_3$:Cr,MgO crystal.

The intensity of line 6 (12 795 cm^{-1}) distinctly increases with pressure. Its pressure coefficient is also linear but it is different from both the pressure coefficients of the R_1 lines and the pressure coefficient of the broadband luminescence and it is equal to −4.3±0.1 cm^{-1}/kbar.

According to the theoretical model and results obtained by Galanciak *et al.*,[19]

$$\frac{dE(\mathrm{Cr}-\mathrm{Cr})}{dp} = \frac{d\Delta_0}{dp} + \frac{d(K_{ex}-K_g)}{dp} + \frac{d(\Theta_{ex}-\Theta_g)}{dp} + 0.5\frac{dJ_{ex}}{dp}[S_{ex}(S_{ex}+1) - 9/2] - 0.5\frac{dJ_g}{dp}[S_g(S_g+1) - 15/2], \quad (1)$$

where Δ_0 is the energy difference between the excited state ^2E and the ground state $^4A_2$ of the single Cr^{3+} ion; K_{ex} and K_g the Coulomb integrals of the excited state ($^4A_2+{}^2E$) and the ground state ($^4A_2+{}^4A_2$) of the Cr^{3+}-Cr^{3+} pair, respectively;

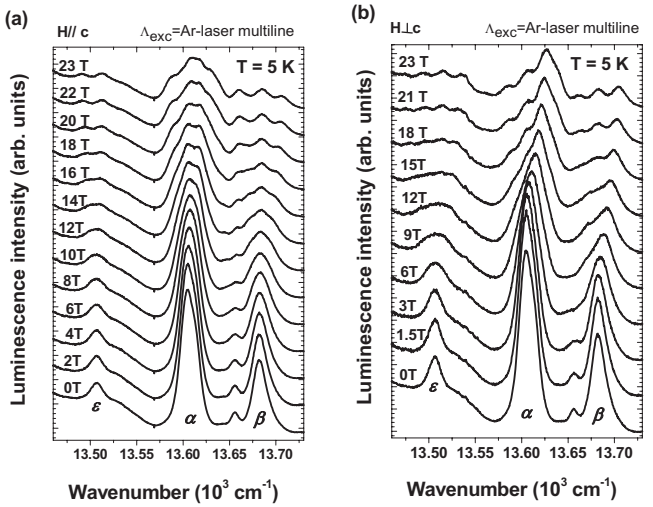

FIG. 9. The spectra of α, β, and ε chromium centers measured at Faraday configuration with the magnetic field directed parallel (a) or perpendicular (b) to the c axis of the crystal.

Θ_{ex} and Θ_g the additional trigonal-field splitting energy of the excited and ground states of the Cr^{3+}-Cr^{3+} pair, respectively; J_{ex} and J_g the exchange integrals of the excited and ground states of the Cr^{3+}-Cr^{3+} pair, respectively; and S_{ex} and S_g the total spin value of the excited and ground states of the Cr^{3+}-Cr^{3+} pair, respectively. S_g can take the values of 0, 1, 2, and 3, whereas S_{ex}: 1 or 2.

Galanciak *et al.* analyzed the case of the extensive studied chromium pairs in ruby, where the needed parameters could be estimated. They got good agreement of the theory with the experimental data for the third and fourth nearest-neighbor pairs. The measured pressure coefficient of R_1 in ruby is equal to −0.76 cm^{-1}/kbar and the pressure coefficients for chromium pairs: −1.5 and −0.86 cm^{-1}/kbar for the $2' \rightarrow 2$ transition of the ferromagnetically coupled third nearest neighbor and $1' \rightarrow 1$ transition of the antiferromagnetically coupled fourth nearest neighbor, respectively.

It is very difficult to perform such analysis in the case of chromium pairs in lithium niobate because such important parameters such as pressure coefficients of the exchange integral, Coulomb integral, and trigonal crystal field splitting are not known. However, comparing the results obtained for ruby we can expect the absolute value of pressure coefficient of the transition related to chromium pairs to be larger from both the value of −1.8 cm^{-1}/kbar of δ center (Cr_{Nb}) and −2.9 cm^{-1}/kbar of γ center (Cr_{Li}). Most probably these centers create the first nearest-neighbor chromium pair in lithium niobate. The measured value of pressure coefficient for line 6 equals to −4.3±0.1 cm^{-1}/kbar, quite close even to the sum of these coefficients for δ and γ centers, then making the assignment of line 6 consistent with this consideration.

C. Magneto-optical studies of single Cr^{3+} ions (α, β, and ε centers)

Placing the Cr^{3+} ions, which have nonzero electronic spin S, into an external magnetic field causes the Zeeman effect,

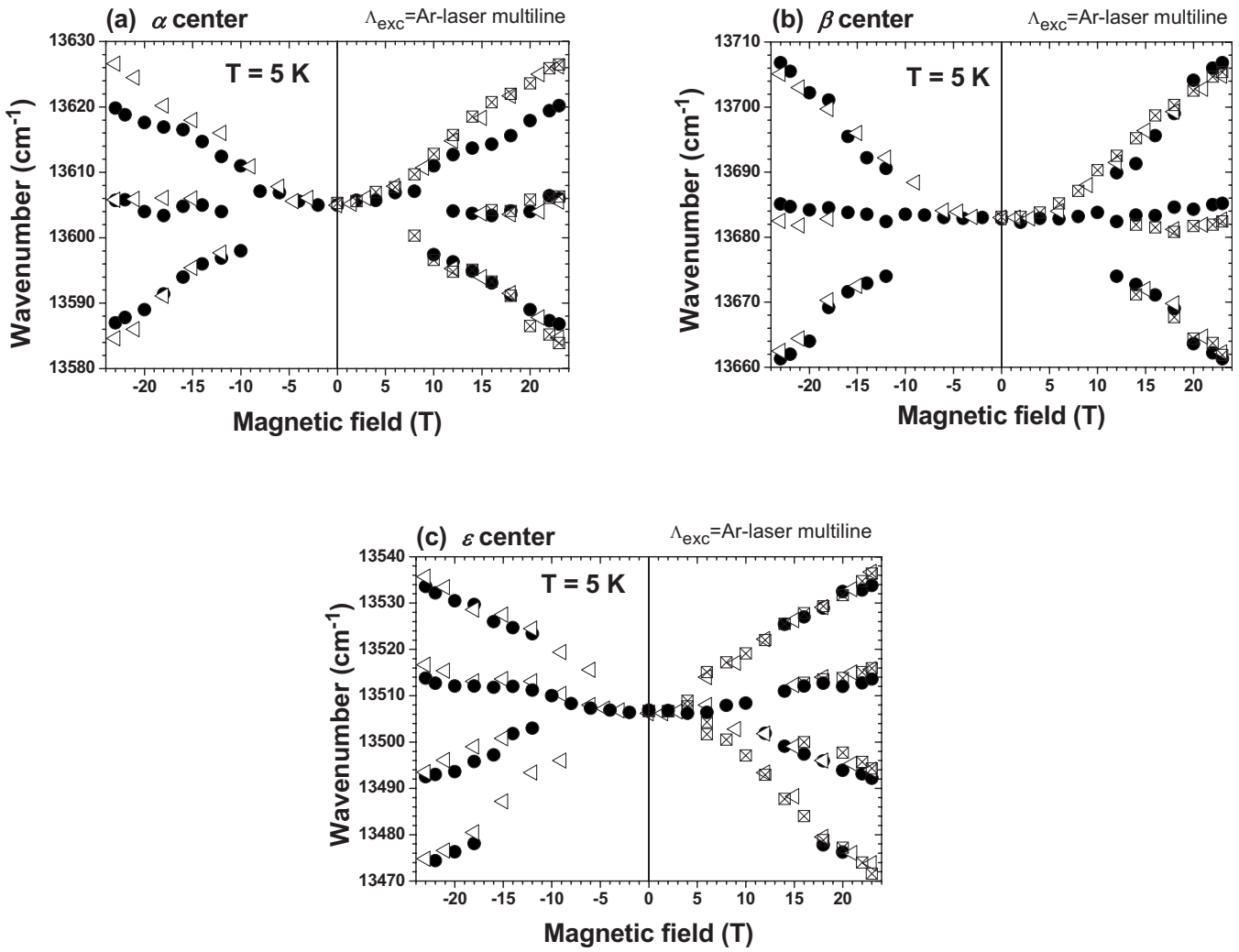

FIG. 10. The spectral positions of the split lines of α, β, and ε centers at temperature $T=5$ K as a function of magnetic field. The closed circles depict results obtained at Faraday configuration with the magnetic field directed parallel to the c axis, open triangles at Faraday configuration with the magnetic field directed perpendicular to the c axis, and crossed squares at Voigt configuration with the magnetic field directed perpendicular to the c axis of the crystal.

i.e., energy level splitting into Zeeman sublevels (see Fig. 8). The energy of the sublevels depends on the value of the S_z component, the magnetic field strength, and on the local symmetry of the ion. The splitting can be determined by the measurements of the luminescence spectra of oriented crystal in a constant magnetic field. The spectra of minority α, β, and ε centers whose R lines were visible at ambient pressure in bulk crystals, measured at Faraday configuration with the magnetic field directed parallel or perpendicular to the c axis, are presented in Figs. 9(a) and 9(b). The magnetic field dependence of the spectral positions of all split lines of these centers is presented in Figs. 10(a)–10(c). Please note that for ε center also the forbidden $S'=-1/2 \rightarrow S=+3/2$ transition was visible.

In general, the spin Hamiltonian including interaction of the chromium ion with the trigonal crystal field with axial symmetry is in the form

$$\mathcal{H} = \beta(\mathbf{HgS}) + D[S_z^2 - 1/3S(S+1)], \tag{2}$$

where $\beta=(e\hbar/2mc)$ is the Bohr magneton; D the zero field splitting, which in lithium niobate is in the range of 0.5 cm^{-1} and therefore the last term can be neglected in our considerations;[2,3,18,20] $\mathbf{H}$ applied external magnetic field; $\mathbf{S}$ total electron spin; and $\mathbf{g}$ tensor of the g factor, which in a ligand field of exact octahedral symmetry is isotropic. In axial symmetry $g_{xx}=g_{yy}=g_{\perp}$; $g_{zz}=g_{\parallel}$. Because of the trigonal distortion of the oxygen octahedral surrounding Cr ions in lithium niobate, the measured values of $g_{\perp}$ and $g_{\parallel}$ can be different and this difference increases when the distortion is stronger.

Assuming the same values of g factor in the ground and excited states we obtain the following dependence of the transition energies on the magnetic field H and on the change of spin projection ΔM_S:

$$\Delta E = g\beta H \Delta M_S, \tag{3}$$

where $g=g_{\|}$ when $H\|c$ or $g=g_{\perp}$ when $H\perp c$ axis of the crystal.

By this technique, the relative slopes of energy levels with magnetic field can be observed and respective values of g factor can be determined. The set of obtained results together with results gained by other authors by EPR measurements is listed in Table I. As we could expect, the differences between $g_{\perp}$ and $g_{\|}$ are the largest for the most distorted α center.

The obtained values of g factor differ a little from those reported in the literature. The most often reported values of g are in the range from 1.96 (Ref. 18) to 1.97 ± 0.001,[4,20–26] for Cr_{Li} or Cr_{Nb} sites and 1.995 ± 0.005 for Cr_{Nb} sites.[4,26] The probable reason is that EPR results concern the majority sites (γ center in green $LiNbO_3$:Cr or δ center in the pink $LiNbO_3$:Cr,Mg crystals)[7] which in the optical experiments give strong broadband luminescence.

D. Magneto-optical studies of Cr^{3+}-Cr^{3+} pairs

The influence of magnetic field on the remaining lines (4–10) occurred to be completely different. The only line sensitive to applied magnetic field was line 4 (13 181 cm^{-1} or 758.7 nm). The splitting patterns of these lines indicate that we are dealing with the transition between excited state with $S'=1$ and the ground state with $S=0$. The splitting is presented in Fig. 11.

In addition at Voigt configuration with the magnetic field directed perpendicular to the c axis of the crystal (then the luminescence is gathered from the direction parallel to the c axis) the twin line at the energy 13 165 cm^{-1}, insensitive to the applied magnetic field, becomes visible. This result indicates that we are dealing with the excited state with $S'=1$ which is split initially by the trigonal crystal field,[27,28] with splitting parameter D equal to 16 cm^{-1}, much larger than D parameters measured for $^4A_2$ state of single chromium ions. The energetic position of the gravity center of the excited state with $S'=1$ is then equal to 13 176 cm^{-1}.

TABLE I. A summary of the parameters of the Cr^{3+} centers in $LiNbO_3$ determined by optical, magneto-optical and EPR measurements.

Cr^{3+} site	Site identification (after Refs. 2 and 7)	$E(^2E)$ R_1 line (cm^{-1})	$g_{\|}$	$g_{\perp}$
α	Li^+ distorted	13 605±1[a,b]	1.76±0.08[a]	2.02±0.10[a]
β	Li^+ distorted	13 683±1[a,b]	2.20±0.10[a]	2.15±0.04[a]
γ	Li^+	13 770±2[b]	1.971±0.002[c,d]	1.971±0.002[c,d]
δ	Nb^{5+}	13 628±6[b]	1.995±0.005[c]	
ε	Nb^{5+} distorted	13 507±1[a,e]	1.98±0.08[a]	1.98±0.08[a]

[a]This work.
[b]Reference 7.
[c]References 4 and 26.
[d]References 24 and 25.
[e]Reference 12.

Performing calculations similar to that described in part B of this paper we have determined components of the g tensor: $g_{\|}=2.10\pm0.03$ and $g_{\perp}=2.09\pm0.04$ which occurred to be isotropic within the experimental error.

All the other lines were completely insensitive to applied magnetic field.

The energy of line 4, the largest in between the set of lines 4–10, indicates, that the ground state with $S=0$ is the lower lying—that means that the coupling is antiferromagnetic. Thus the next observed transition, the strongest line 6 (12 795 cm^{-1}), corresponds to the $S'=1\rightarrow S=1$ transition. Such attribution is reasonable taking into account that for the exchange induced electric dipole transitions in a first approximation the selection rule $\Delta S=0$, $\Delta M_S=0$ obeys.[16,28–30] This is the reason why for these lines no influence of magnetic field can be observed. The only observed transition with $\Delta S=1$ (line 4) is much weaker and has other polarization, which can be seen in Fig. 3.[31]

Lines 7 and 8 (12 530 cm^{-1} and the pair of lines at energies 12 232 and 12 198 cm^{-1}) seem to be the vibrational sidebands of line 6. Their energetic distances to line 6 are similar to the energetic distances of phonon replicas of the R_1 lines of the main γ and δ centers observed at high pressures (see Fig. 12). This conclusion is also supported by the observation of the same decay times for lines 6–8.

The pattern of line 9 (11 993 cm^{-1}) corresponds to the $S'=2\rightarrow S=2$ transition, also with $\Delta M_S=0$ and the energy of line 10 (11 993 cm^{-1}) indicates that it is first phonon replica of this transition.

The energetic structure of the ground state of chromium pair system is described by the exchange interaction. However, it can be seen that the Lande interval rule is not obeyed. Much better agreement with experiment would be obtained if we concern biquadratic contribution to the isotropic Cr-Cr interaction. Then the Hamiltonian is in the form[27,32,33]

$$\mathcal{H}_{ex}(^4A_2 + {}^4A_2) = J\mathbf{S}_1\mathbf{S}_2 + j(\mathbf{S}_1\mathbf{S}_2)^2, \tag{4}$$

where J is isotropic exchange coupling parameter, j biquadratic term describing the separation between the spin multiplets (if $\mathbf{S}_1$, $\mathbf{S}_2>1/2$); and $\mathbf{S}_1$ and $\mathbf{S}_2$ total electron spins of ions 1 and 2, respectively, equal to 3/2.

This gives a modified interval rule as follows:

$$E_S - E_{S-1} = JS + jS[S^2 - S_1(S_1+1) - S_2(S_2+1)]. \tag{5}$$

Fitting the observed ground-state splittings to Eq. (5) we get J and j parameters equal to 481 and 15 cm^{-1}, respectively.

The obtained values for the first sight seem to be very large. However, we could expect the strongly antiferromagnetic interaction as the result of the approximately linear Cr^{3+}-O^{2-}-Cr^{3+} bonds.[34] The almost strictly obeying $\Delta M_S=0$ rule is also connected with the large value of the coupling constant J. For this reason also chromium pairs are not observed in EPR: for $J\geqslant 400$ cm^{-1} they are in nonparamagnetic singlet state even at room temperature and only the pairs of the second and third orders with the isotropic exchange coupling parameter $J\approx 1.5$ cm^{-1} are observed.[18,35,36]

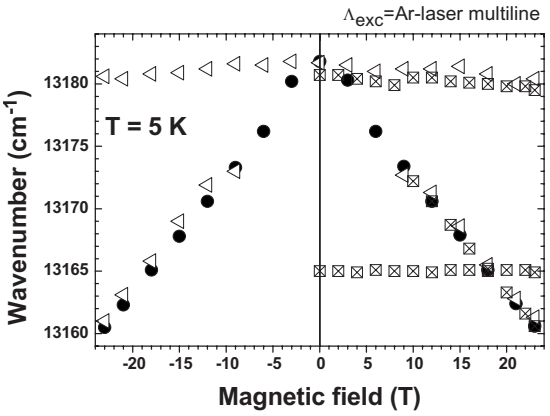

FIG. 11. The spectral positions of line 4 (13 180 cm^{-1} or 758.7 nm) at temperature $T=5$ K as a function of magnetic field. The closed circles depict results obtained at Faraday configuration with the magnetic field directed parallel to the c axis, open triangles at Faraday configuration with the magnetic field directed perpendicular to the c axis, and crossed squares at Voigt configuration with the magnetic field directed perpendicular to the c axis of the crystal.

The energetic structure of the excited state in which one of the paired ions is raised to the ^2E state is more complicated. Because of the existence of trigonal-field spin-orbit splitting of the isolated Cr^{3+} ion (equal to 17 or 38 cm^{-1} for the δ or γ center, respectively), which in this case can be of the same order as the excited-state exchange coupling, both perturbations to the zero order Hamiltonian have to be considered simultaneously.[14,15,30,31,34,37–39] A more general exchange Hamiltonian is of the form

$$\mathcal{H}_{ex}(^2E + {}^4A_2) = \Sigma J_{1i,2k}\mathbf{s}_{1i}\mathbf{s}_{2k}, \tag{6}$$

where $\mathbf{s}_1$ and $\mathbf{s}_2$ are spins of electrons on ions 1 and 2, respectively, and i and k run over the three one-electron t_{2g}

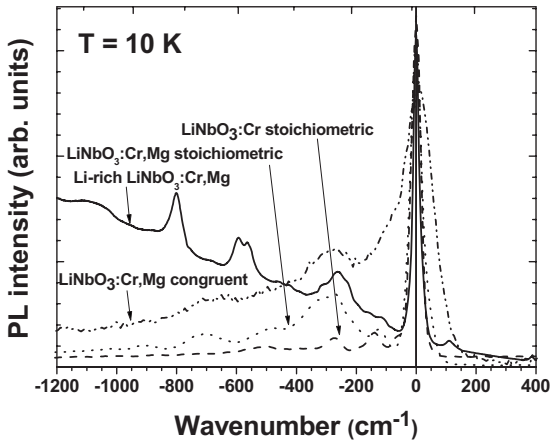

FIG. 12. Comparison of effective phonon energies of chromium pairs with effective phonon energies of γ and δ centers observed at high pressures (135 kbar for the γ center of stoichiometric $LiNbO_3$:Cr, 149 kbar for the δ center of stoichiometric $LiNbO_3$:Cr, Mg, and 154 kbar for the δ center of congruent $LiNbO_3$:Cr, Mg crystal). The zero point of all the lines is moved to the respective zero-phonon line.

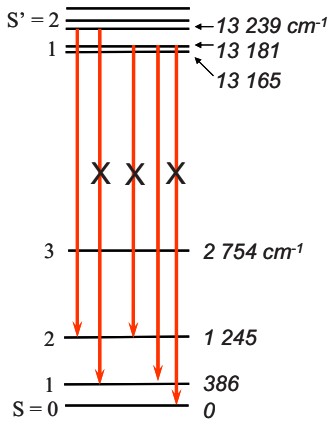

FIG. 13. (Color online) Energy level diagram of Cr^{3+}-Cr^{3+} pair system with marked spin allowed and forbidden transitions in the $LiNbO_3$:Cr^{3+},MgO crystal containing excess of Li^+ ions.

orbitals on each ion; and $J_{1i,2k}$ is a measure of exchange between the ith orbital of ion 1 and the jth orbital of ion 2.

For simplicity the biquadratic term was here omitted. The detailed analysis of its contribution to the excited-state energy level scheme in the case of chromium pairs in ruby is given in Ref. 31.

The exact excited-state energy level scheme of chromium pairs in the Li-rich $LiNbO_3$:Cr,Mg crystal cannot be established on the base of our data; however, we could determine the distance between one level of the $S'=1$ state and lowest lying of the levels with $S'=2$. Then we can construct the estimated level scheme which is presented in Fig. 13.

IV. CONCLUSIONS

Li-rich $LiNbO_3$:Cr,MgO crystal has some advantage over the near-stoichiometric $LiNbO_3$:Cr,MgO or $LiNbO_3$:Cr crystals from the point of studying chromium pairs in this material. Its important property is much more balanced chromium ion distribution between lithium and niobium crystal sites compared with $LiNbO_3$:Cr,MgO where chromium occupies mainly niobium sites, and $LiNbO_3$:Cr where chromium occupies mainly lithium sites. Thus the creation of nearest-neighbor Cr_{Li}-Cr_{Nb} pairs was much more probable and optical measurements of these pairs could be performed even on microscopic samples inserted into high-pressure diamond-anvil cell.

High-pressure and magneto-optical studies of this crystal allow us to conclude that indeed the relatively narrow lines observed in the range of 750–860 nm (13 300–11 600 cm^{-1}) are related to the antiferromagnetically exchange-coupled Cr^{3+}-Cr^{3+} pairs, where line at 13 181 cm^{-1} corresponds to the $1' \rightarrow 0$ transition, line at 12 795 cm^{-1} corresponds to the $1' \rightarrow 1$ transition, line at 11 993 cm^{-1} corresponds to the $2' \rightarrow 2$ transition, and the rest of lines are the vibrational sidebands of the main $1' \rightarrow 1$ and $2' \rightarrow 2$ transitions.

The only unidentified line remains the weak line number 5 of energy about 12 904 cm^{-1}.

TABLE II. A summary of the parameters describing Cr^{3+}-Cr^{3+} pairs in Li-rich $LiNbO_3$:Cr,MgO crystal determined by optical, high-pressure, and magneto-optical measurements.

Line number (see the text)	Line position	Identification	Decay time at $T=10$ K (μs)	dE/dp (cm^{-1}/kbar)	$g_{\parallel}$	$g_{\perp}$	Comments
4	13 165 cm^{-1} +13 181 cm^{-1}	Cr^{3+}-Cr^{3+} $S'=1\rightarrow S=0$			2.10±0.03	2.09±0.04	$D=16$ cm^{-1} $J\sim 481$ cm^{-1} $j\sim 15$ cm^{-1}
6	12 795 cm^{-1}	Cr^{3+}-Cr^{3+} $S'=1\rightarrow S=1$	39±2	−4.3±0.1			No splitting $\Delta M_s=0$
7	≈12 530 cm^{-1}	Vibrational sidebands	39±4				No splitting
8	12 232 cm^{-1} +12 198 cm^{-1}	Vibrational sidebands	39±4				No splitting
9	11 993 cm^{-1}	Cr^{3+}-Cr^{3+} $S'=2\rightarrow S=2$	31±2				No splitting $\Delta M_s=0$
10	≈11 726 cm^{-1}	Vibrational sidebands					No splitting

The summary of obtained results concerning these lines is listed in Table II.

According to magneto-optical results these pairs occurred to be very strongly antiferromagnetically coupled. We determined the isotropic exchange coupling parameter J equal to 481 cm^{-1} and biquadratic term j equal to 15 cm^{-1}. Such large values are hardly ever reported for chromium ions: in the case of first nearest-neighbor Cr^{3+} pairs in Al_2O_3 $J\approx 225-240$ cm^{-1} (Refs. 14, 31, and 38), in $LaAlO_3$ $J\approx 67-69$ cm^{-1} (Refs. 16 and 30), in $YAlO_3$ $J\approx 26$ cm^{-1} (Ref. 34), and in $Be_3Al_2Si_6O_{18}$—only 2.26 cm^{-1} (Ref. 40). The J value of this range was predicted for $LiNbO_3$:Cr on the base of the EPR results by Siu *et al.*[18] and Grachev *et al.*[35] However, they could not determine it because of the impossibility of observation nonparamagnetic singlet states by EPR. Our result is consistent with these predictions.

To the authors' knowledge such strong or even stronger coupling was observed so far only in chlorides containing copper. The reported values of isotropic exchange coupling parameter J are equal from 550 to 885 cm^{-1} for different salts.[41]

ACKNOWLEDGMENTS

This work was partially supported by a research grant of the Polish Ministry of Science and Higher Education for years 2006–2009. Magneto-optical experiments were performed during the stay of A.K. in Grenoble High Magnetic Field Laboratory through the support of the European Community from Contract No. RITA-CT-2003-505474, which is highly appreciated by the authors.

*Present address: Department of Technology, GAIKER Technological Centre, 48170 Zamudio, Spain.

[1] L. Arizmendi, Phys. Status Solidi A **201**, 253 (2004).
[2] P. I. Macfarlane, K. Holliday, J. F. H. Nicholls, and B. Henderson, J. Phys.: Condens. Matter **7**, 9643 (1995).
[3] J. Díaz-Caro, J. García-Solé, D. Bravo, J. A. Sanz-García, F. J. López, and F. Jaque, Phys. Rev. B **54**, 13042 (1996).
[4] V. Grachev and G. Malovichko, Phys. Rev. B **62**, 7779 (2000), and references therein.
[5] A. Kamińska, J. E. Dmochowski, A. Suchocki, J. Garcia-Sole, F. Jaque, and L. Arizmendi, Phys. Rev. B **60**, 7707 (1999).
[6] A. Kamińska, A. Suchocki, M. Grinberg, J. Garcia-Sole, F. Jaque, and L. Arizmendi, J. Lumin. **87-89**, 571 (2000).
[7] A. Kamińska, A. Suchocki, L. Arizmendi, D. Callejo, F. Jaque, and M. Grinberg, Phys. Rev. B **62**, 10802 (2000).
[8] S. A. Basun, G. M. Salley, A. A. Kaplyanskii, K. Polgar, H. G. Gallagher, L. Lu, and U. Happek, J. Lumin. **83-84**, 435 (1999).
[9] G. M. Salley, S. A. Basun, A. A. Kaplyanskii, R. S. Meltzer, K. Polgar, and U. Happek, J. Lumin. **87-89**, 1133 (2000).
[10] V. Trepakov, A. Skvortsov, S. Kapphan, L. Jastrabik, and V. Vorlicek, Ferroelectrics **239**, 297 (2000).
[11] M. D. Serrano, V. Bermudez, L. Arizmendi, and E. Dieguez, J. Cryst. Growth **210**, 670 (2000).
[12] T. P. J. Han, F. Jaque, L. Arizmendi, V. Bermúdez, A. Suchocki, A. Kamińska, and S. Kobyakov, Phys. Rev. B **68**, 132103 (2003).
[13] J. Ferguson and B. van Oosterhout, J. Lumin. **18-19**, 165 (1979).
[14] R. C. Powell and B. DiBartolo, Phys. Status Solidi A **10**, 315 (1972).
[15] M. Naito, J. Phys. Soc. Jpn. **34**, 1491 (1973).
[16] J. Heber, K. H. Hellwege, S. Leutloff, and W. Platz, Z. Phys. **246**, 261 (1971).

[17] T. H. Yeom, Y. M. Chang, C. Rudowicz, and S. H. Choh, Solid State Commun. **87**, 245 (1993).
[18] G. G. Siu and Zhao Min-Guang, Phys. Rev. B **43**, 13575 (1991).
[19] D. Galanciak, S. Łegowski, H. Męczyńska, and M. Grinberg, J. Phys. IV **4**, C4-565 (1994).
[20] Zi-Y. Yang, C. Rudowicz, and J. Qin, Physica B **318**, 188 (2002).
[21] M. G. Zhao and Y. Lei, J. Phys.: Condens. Matter **9**, 529 (1997).
[22] G. Burns, D. F. O'Kane, and R. S. Title, Phys. Rev. **167**, 314 (1967).
[23] D. G. Rexford, Y. M. Kim, and H. S. Story, J. Chem. Phys. **52**, 860 (1970).
[24] G. Corradi, H. Söthe, J. M. Spaeth, and K. Polgar, J. Phys.: Condens. Matter **3**, 1901 (1991).
[25] A. Martin, F. J. López, and F. Agulló-López, J. Phys.: Condens. Matter **4**, 847 (1992).
[26] G. Malovichko, V. Grachev, A. Hofstaetter, E. Kokanyan, A. Scharmann, and O. Schirmer, Phys. Rev. B **65**, 224116 (2002).
[27] A. Abragam and B. Bleaney, *Electron Paramagnetic Resonance of Transition Ions* (Clarendon, Oxford, 1970).
[28] L. M. Kanskaya and A. K. Przhewuskii, Opt. Spektrosk. **26**, 226 (1969) [Opt. Spectrosc. **26**, 121 (1969)].
[29] L. M. Kanskaya, W. W. Druzhinin, and A. K. Przhewuskii, Solid State Phys. **11**, 2595 (1969).
[30] J. P. van der Ziel, Phys. Rev. B **4**, 2888 (1971).
[31] J. P. van der Ziel, Phys. Rev. B **9**, 2846 (1974).
[32] E. A. Harris and J. Owen, Phys. Rev. Lett. **11**, 9 (1963).
[33] D. S. Rodbell, I. S. Jacobs, J. Owen, and E. A. Harris, Phys. Rev. Lett. **11**, 10 (1963).
[34] J. P. van der Ziel, J. Chem. Phys. **57**, 2442 (1972).
[35] V. Grachev, G. Malovichko, and W. W. Trotskii, Solid State Phys. **29**, 607 (1987).
[36] V. Grachev, G. Malovichko, and O. Schirmer, Ferroelectrics **185**, 5 (1996).
[37] A. E. Nikiforov and V. I. Cherepanov, Phys. Status Solidi **14**, 391 (1966).
[38] P. Kisliuk, N. C. Chang, P. L. Scott, and M. H. L. Pryce, Phys. Rev. **184**, 367 (1969).
[39] J. P. van der Ziel, Phys. Rev. Lett. **26**, 766 (1971).
[40] A. Edgar and D. R. Huston, J. Phys. C **11**, 5051 (1978).
[41] J. Owen and E. A. Harris, in *Electron Paramagnetic Resonance*, edited by S. Geschwind (Plenum, New York, 1972), Chap. 6.